



# Luminescent cadmium phenylenediacetate coordination polymers with bis(pyridylformyl)piperazine tethers: Influence of pendant arm position on topology

Curtis Y. Wang<sup>a</sup>, Robert L. LaDuca<sup>b,\*</sup>

<sup>a</sup> Diamond Bar High School, Diamond Bar, CA 91765, USA

<sup>b</sup> Lyman Briggs College and Department of Chemistry, E-30 Holmes Hall, Michigan State University, East Lansing, MI 48825, USA

## ARTICLE INFO

### Article history:

Received 11 August 2010

Received in revised form 26 August 2010

Accepted 26 August 2010

Available online 17 September 2010

### Keywords:

Cadmium

Coordination polymer

Dicarboxylate

Luminescence

Hydrogen bonding

## ABSTRACT

Hydrothermal synthesis has generated divalent cadmium coordination polymers containing phenylenediacetate (phda) and bis(4-pyridylformyl)piperazine (bpfp) ligands, in which the position of the pendant acetate arms plays a very significant role in structure direction during self-assembly.  $[\text{Cd}(1,2\text{-Hphda})_2(4\text{-bpfp})]_n$  (**1**) exhibits 2-D polymeric layers with embedded *anti-syn* bridged  $[\text{Cd}(\text{OCO})_2]_n$  ribbons.  $\{[\text{Cd}(1,3\text{-phda})(4\text{-bpfp})(\text{H}_2\text{O})_2]_n$  (**2**) has crystallographically independent (4,4) grids with different carboxylate binding modes, engaged in parallel interpenetration.  $\{[\text{Cd}(1,4\text{-phda})(4\text{-bpfp})(\text{H}_2\text{O})]_n$  (**3**) manifests acentric 1-D chains with an uncommon 4-connected  $3^34^25$  topology instilled by the mismatch in ligand length. Luminescent properties of all phases are also reported.

© 2010 Elsevier B.V. All rights reserved.

## 1. Introduction

The design and characterization of crystalline coordination polymer solids remains a popular basic research interest because of these materials' growing industrially important applications [1] such as gas storage [2], selective adsorption and separation [3], ion exchange [4], heterogeneous catalysis [5], luminescence [6], and second harmonic generation [7]. Among most common ligands used in the design of these solids are aromatic dicarboxylates such as terephthalate [8] or isophthalate (ip) [9], which instill both the structural components and charge balance crucial for the self-assembly of crystalline frameworks. Variations both in metal coordination environment and carboxylate group binding mode promote a wide scope of accessible structural topologies in aromatic dicarboxylate coordination polymers [10]. The lack of crystal field stabilization in  $d^{10}$  configuration divalent cadmium ions allows the specific coordination environment to respond to the geometric and steric requirements of the carboxylate ligands during self-assembly [11]. Additionally the absence of  $d-d$  transitions with this ion provides the necessary spectral window for visible light fluorescence [6a].

More recently, aromatic dicarboxylates with conformationally flexible pendant arms such as isomeric phenylenediacetate (phda)

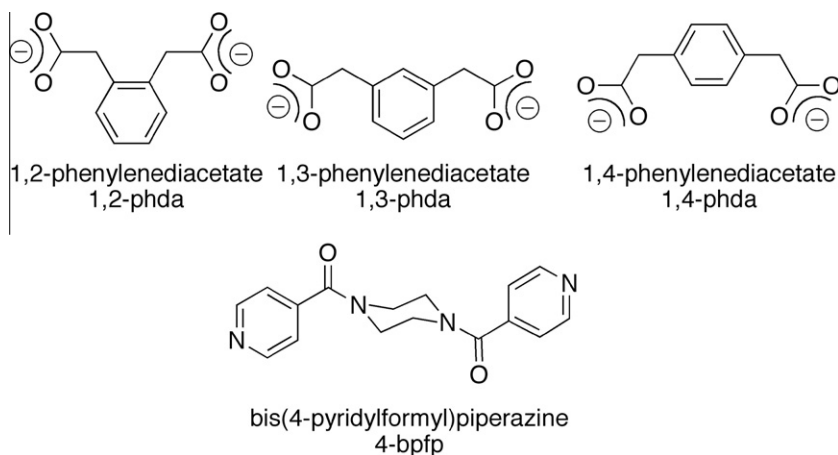
\* Corresponding author. Tel.: +1 517 432 2268.

E-mail address: [laduca@msu.edu](mailto:laduca@msu.edu) (R.L. LaDuca).

ligands (Scheme 1) have been employed in order to construct coordination polymers whose topologies vary from those obtained with more rigid carboxylate groups [12–14]. A series of divalent cobalt coordination polymers with phda and bis(4-pyridylmethyl)piperazine (4-bpmp) ligands reveals the critical dependence of carboxylate pendant arm position on the final structural topology [15].  $\{[\text{Co}(1,4\text{-phda})(4\text{-bpmp})(\text{H}_2\text{O})_2] \cdot 2\text{H}_2\text{O}\}_n$  presents a layered structure with standard (4,4) grid topology, while  $[\text{Co}(1,3\text{-phda})(4\text{-bpmp})]_n$  has  $[\text{Co}(1,3\text{-phda})]_n$  layers with embedded  $\{\text{Co}_2(\text{CO}_2)_2\}$  dinuclear units pillared by 4-bpmp ligands into a 3-D primitive cubic topology. The *ortho*-substituted 1,2-phda derivative  $\{[\text{Co}(1,2\text{-phda})(4\text{-bpmp})_{1.5}(\text{H}_2\text{O})](\text{H}_2\text{O})_{0.5}(\text{ClO}_4) \cdot 12\text{H}_2\text{O}\}_n$  manifests a unique 5-connected network with an Archimedean topology consisting of triangular and rectangular circuits.

Similarly, divalent zinc phda coordination polymer phases with neutral 4,4-dipyridylamine (dpa) tethers exhibit divergent topologies depending on the geometric disposition of the acetate groups. Although  $\{[\text{Zn}(1,4\text{-phda})(\text{dpa})] \cdot \text{H}_2\text{O}\}_n$  shows a simple (4,4) corrugated layer grid structure,  $\{[\text{Zn}(1,2\text{-phda})(\text{dpa})] \cdot 2\text{H}_2\text{O}\}_n$  and  $[\text{Zn}(1,3\text{-phda})(\text{dpa})]_n$  possess fourfold interpenetrated  $4^26^38$  SrAl<sub>2</sub> and  $6^6$  diamondoid 3-D networks respectively [16].

In this contribution we investigate the effect of acetate arm disposition on the topology of cadmium phda coordination polymers incorporating the bis(4-pyridylformyl)piperazine (4-bpfp) neutral tethering ligand (Scheme 1). This dipodal dipyrindyl ligand has seldom been used in coordination chemistry [17], especially with



Scheme 1. Ligands used in this study.

dicarboxylate anionic components [18]. Mixed-ligand extended solid phases with all three phda isomers have been obtained via hydrothermal synthesis and structurally characterized.  $\{[Cd(1,2\text{-Hphda})_2(4\text{-bpfp})]\cdot 2H_2O\}_n$  (**1**),  $\{[Cd(1,3\text{-phda})(4\text{-bpfp})(H_2O)]_2\}_n$  (**2**) and  $\{[Cd(1,4\text{-phda})(4\text{-bpfp})(H_2O)]\}_n$  (**3**) possesses different 1-D and 2-D topologies. Luminescent properties of these new materials are also reported herein.

## 2. Experimental section

### 2.1. General considerations

Cadmium salts and dicarboxylic acids were obtained commercially from Aldrich. Bis(4-pyridylformyl)piperazine (4-bpfp) was prepared via modification of a published procedure [17]. Pyridine was refluxed with  $CaH_2$  under flowing  $N_2$  and distilled immediately prior to use. Water was deionized above  $3\text{ M}\Omega\text{ cm}$  in-house. Elemental analysis was performed by Micro-Analysis, Inc., Wilmington, Delaware, USA. IR spectra Infrared spectra were recorded on powdered samples on a Perkin Elmer Spectrum One instrument. The luminescence spectra were obtained with a Hitachi F-4500 Fluorescence Spectrometer on solid crystalline samples anchored to quartz microscope slides with Rexon Corporation RX-22P ultra-violet-transparent epoxy adhesive.

### 2.2. Preparation of $\{[Cd(1,2\text{-Hphda})_2(4\text{-bpfp})]\cdot 2H_2O\}_n$ (**1**)

$Cd(NO_3)_2\cdot 4H_2O$  (29.9 mg, 0.0972 mmol), 4-bpfp (28.7 mg, 0.0972 mmol), 1,2-phenylenediacetic acid (18.9 mg, 0.0972 mmol), and 7 mL deionized water were placed into a 23 mL Teflon-lined acid digestion bomb. The bomb was sealed and heated in an oven at  $120\text{ }^\circ\text{C}$  for 48 h, and then cooled slowly to  $25\text{ }^\circ\text{C}$ . Colorless blocks of **1** (8 mg, 0.01 mmol, 21% yield based on the limiting reactant 1,2-phenylenediacetic acid) were isolated after washing with distilled water, ethanol, and acetone and drying in air. Anal. Calc. for  $C_{36}H_{34}CdN_4O_{10}$  **1**: C, 54.38; H, 4.31; N, 7.05% Found: C, 54.11; H, 4.28; N, 7.00%. IR ( $cm^{-1}$ ): 2921 (w), 1708 (s), 1637 (s), 1615 (w), 1567 (s), 1504 (w), 1464 (w), 1435 (w), 1412 (w), 1357 (s), 1267 (s), 1224 (w), 1191 (s), 1169 (s), 1101 (w), 1064 (w), 1041 (w), 1006 (m), 910 (w), 895 (w), 860 (w), 843 (m), 819 (w), 772 (m), 736 (w), 716 (w), 688 (s), 661 (w).

### 2.3. Preparation of $\{[Cd(1,3\text{-phda})(4\text{-bpfp})(H_2O)]_2\}_n$ (**2**)

$Cd(NO_3)_2\cdot 4H_2O$  (29.9 mg, 0.0972 mmol), 4-bpfp (28.7 mg, 0.0972 mmol), 1,3-phenylenediacetic acid (18.9 mg, 0.0972 mmol),

1 mL of 1.0 M NaOH and 5 mL deionized water were placed into a 15 mL screw-cap vial. The vial was sealed and heated in an oil bath at  $90\text{ }^\circ\text{C}$  for 48 h, and then cooled slowly to  $25\text{ }^\circ\text{C}$ . Colorless blocks of **2** (20 mg, 0.032 mmol, 32% yield based on Cd) were isolated after washing with distilled water, ethanol, and acetone and drying in air. Anal. Calc. for  $C_{52}H_{52}Cd_2N_8O_{14}$  **2**: C, 50.46; H, 4.23; N, 9.05% Found: C, 50.17; H, 4.09; N, 8.96%. IR ( $cm^{-1}$ ): 3400 (w, br) 2995 (w), 2870 (w), 2323 (w), 1633 (s), 1606 (s), 1556 (m), 1499 (w), 1470 (m), 1438 (m), 1416 (m), 1363 (s), 1330 (w), 1286 (s), 1261 (s), 1219 (w), 1162 (w), 1054 (w), 1006 (s), 968 (w), 933 (w), 905 (w), 872 (w), 837 (s), 785 (w), 759 (w), 716 (w), 678 (w).

### 2.4. Preparation of $[Cd(1,4\text{-phda})(4\text{-bpfp})(H_2O)]_n$ (**3**)

$Cd(NO_3)_2\cdot 4H_2O$  (29.9 mg, 0.0972 mmol), 4-bpfp (28.7 mg, 0.0972 mmol), 1,3-phenylenediacetic acid (18.9 mg, 0.0972 mmol), 1 mL of 1.0 M NaOH and 5 mL deionized water were placed into a 15 mL screw-cap vial. The vial was sealed and heated in an oil bath at  $90\text{ }^\circ\text{C}$  for 48 h, and then cooled slowly to  $25\text{ }^\circ\text{C}$ . Colorless blocks of **3** (27 mg, 0.043 mmol, 45% yield based on Cd) were isolated after washing with distilled water, ethanol, and acetone and drying in air. Anal. Calc. for  $C_{26}H_{26}CdN_4O_7$  **3**: C, 50.46; H, 4.23; N, 9.05% Found: C, 50.03; H, 4.47; N, 8.89%. IR ( $cm^{-1}$ ): 3110 (w, br), 1708 (w), 1638 (s), 1607 (m), 1577 (s), 1497 (w), 1463 (m), 1436 (m), 1402 (m), 1362 (m), 1325 (w), 1288 (s), 1262 (s), 1211 (w), 1262 (s), 1211 (w), 1162 (w), 1101 (w), 1006 (s), 948 (w), 903 (w), 841 (m), 762 (m), 746 (w), 705 (w), 665 (w).

## 3. X-ray crystallography

Single-crystal diffraction data for **1–3** were collected using a Bruker-AXS Apex2 CCD instrument. Diffraction data was acquired using graphite-monochromated Mo  $K\alpha$  radiation ( $\lambda = 0.71073\text{ \AA}$ ). The diffraction data were integrated with SAINT [19]. Lorentz and polarization effect and empirical absorption corrections were applied with SADABS [20]. The structures were solved using direct methods and refined on  $F^2$  using SHELXTL [21]. All non-hydrogen atoms were refined with anisotropic thermal parameters. Hydrogen atoms bound to carbon atoms were placed in calculated positions and refined with isotropic thermal parameters using a riding model. Hydrogen atoms bound to water molecules were located by Fourier difference map and restrained at fixed positions. Enantiomeric purity within the crystal of **3** is confirmed by the Flack parameter [22] of 0.00(3). Disorder within the piperaziny rings of the 4-bpfp ligands in **1** was modeled successfully with partial

occupancies. Relevant crystallographic data for **1–3** are listed in Table 1.

## 4. Results and discussion

### 4.1. Synthesis and spectral characterization

Hydrothermal reaction of cadmium nitrate, the requisite dicarboxylic acid, and bis(4-pyridylformyl)piperazine generated crystalline samples of **1–3**. The infrared spectra of **1–3** were consistent with their single crystal structures. Features between  $\sim 1620$  and  $\sim 1640$   $\text{cm}^{-1}$  in all cases reveal the presence of the C=O formyl group within the 4-bpfp ligands. Sharp, medium intensity bands in the range of  $\sim 1600$   $\text{cm}^{-1}$  to  $\sim 1200$   $\text{cm}^{-1}$  are attributed to stretching modes of the pyridyl rings of the 4-bpfp ligands and the aromatic rings of the dicarboxylate ligands. Features corresponding to pyridyl ring puckering modes are evident in the region between  $\sim 930$  and  $\sim 600$   $\text{cm}^{-1}$ . Asymmetric and symmetric C–O stretching modes of the fully deprotonated dicarboxylate ligands are present as broadened bands at  $1567$   $\text{cm}^{-1}$  and  $1357$   $\text{cm}^{-1}$  (**1**),  $1606$   $\text{cm}^{-1}$  and  $1363$   $\text{cm}^{-1}$  (**2**), and  $1577$   $\text{cm}^{-1}$  and  $1402$   $\text{cm}^{-1}$  (**3**). Broad, weak spectral features at  $\sim 3100$ – $3400$   $\text{cm}^{-1}$  (O–H stretching modes) denote the presence of the aqua ligands in **2** and **3**. The peak at  $1708$   $\text{cm}^{-1}$  in the spectrum of **1** is indicative of C–O stretching within the protonated carboxylate groups of the 1,2-Hphda ligands.

### 4.2. Structural description of $[\text{Cd}(1,2\text{-Hphda})_2(4\text{-bpfp})]_n$ (**1**)

The asymmetric unit of compound **1** contains a divalent cadmium ion located on a crystallographic inversion center, one singly protonated 1,2-Hphda ligand, and one-half of a 4-bpfp molecule whose central piperazinyl ring and formyl oxygen atoms are disordered equally over two positions. A slightly distorted  $\{\text{CdO}_4\text{N}_2\}$  octahedral coordination sphere exists at cadmium, with *trans* pyr-

idyl nitrogen donor atoms from two 4-bpfp ligands in the axial positions and single oxygen atom donors from four different 1,2-Hphda ligands in the equatorial plane (Fig. S1). Bond lengths and angles around cadmium are listed in Table 2.

One carboxylate terminus of every 1,2-Hphda ligand bridges two cadmium atoms in an *anti-syn* bridging mode, constructing  $[\text{Cd}(1,2\text{-Hphda})_2]_n$  ribbons aligned along the  $[100]$  crystal direction (Fig. 1a). Eight-membered  $[\text{Cd}(\text{OCO})_2]$  rings are joined in a *spiro* fashion within the center of the ribbon motifs, with a Cd...Cd contact distance of  $5.174$  Å. Each pair of cadmium atoms is bridged by deprotonated acetate groups belonging to two 1,2-Hphda ligands, with the protonated acetate arms projecting towards the exterior of the  $[\text{Cd}(1,2\text{-Hphda})_2]_n$  ribbons.

Adjacent ribbon motifs are pillared into 2-D  $[\text{Cd}(1,2\text{-Hphda})_2(4\text{-bpfp})]_n$  coordination polymer layers (Fig. 1b) by *anti*-conformation 4-bpfp tethering ligands, which span a Cd...Cd distance of  $16.753$  Å. If both carboxylate groups spanning each pair of cadmium atoms are considered a single linkage, the layer motif can be simplified as a 4-connected (4,4) nearly perfect rectangular grid, with Cd...Cd...Cd angles of  $89.7^\circ$  and  $90.3^\circ$ . Individual layers lie along the  $(011)$  crystal planes and aggregate into 3-D (Fig. S2) by hydrogen bonding donation from the protonated pendant acetate groups to oxygen atoms of ligated acetate moieties, resulting in a 6-connected primitive cubic supramolecular topology. Hydrogen bonding information is given in Table 3.

### 4.3. Structural description of $\{[\text{Cd}(1,3\text{-phda})(4\text{-bpfp})(\text{H}_2\text{O})_2]_n$ (**2**)

The large asymmetric unit of compound contains two crystallographically independent sets, each containing a divalent cadmium atom, a 1,3-phda ligand, a 4-bpfp ligand, and a ligated water molecule (Fig. S3). Cd1 displays a distorted  $\{\text{CdN}_2\text{O}_5\}$  pentagonal bipyramidal geometry, with the axial positions taken up by 4-bpfp pyridyl nitrogen donors and the equatorial plane filled by an aqua ligand and chelating carboxylate groups from two 1,3-phda ligands. In contrast Cd2 possesses a distorted  $\{\text{CdN}_2\text{O}_4\}$  octahedral geometry. As seen for Cd1, 4-bpfp pyridyl nitrogen atoms are disposed in a *trans* fashion. The remaining four coordination sites are occupied by an aqua ligand, a chelating 1,3-phda carboxylate group, and a single oxygen atom from a monodentate 1,3-phda carboxylate terminus. A long Cd...O interaction ( $2.773(4)$  Å) supplements the octahedral coordination environment at Cd2. Crystallographic independence is thereby enforced by the differing coordination environments at Cd1 and Cd2 and binding mode of the 1,3-phda ligands. Bond lengths and angles within the independent coordination environments in **2** are listed in Table 4.

Cd1 atoms are connected into zig-zag  $[\text{Cd}(1,3\text{-phda})(\text{H}_2\text{O})]_n$  chains, oriented along the  $[101]$  crystal direction, by bis(chelating) 1,3-phda ligands. Cd2 atoms are linked into similar  $[\text{Cd}(1,3\text{-phda})(\text{H}_2\text{O})]_n$  chains by 1,3-phda ligands in a monodentate/chelating binding mode (Fig. 2). The respective Cd...Cd through-ligand contact distances within the crystallographically distinct chain patterns are  $12.204$  and  $12.308$  Å. Different binding modes are reflected in different C–C...C–C torsion angles between the 1,3-phda acetate arms ( $160.9^\circ$  and  $144.4^\circ$ , respectively). Both types of chains are

**Table 1**  
Crystal and structure refinement data for **1–3**.

Compound	<b>1</b>	<b>2</b>	<b>3</b>
Empirical formula	$\text{C}_{36}\text{H}_{34}\text{CdN}_4\text{O}_{10}$	$\text{C}_{52}\text{H}_{52}\text{Cd}_2\text{N}_8\text{O}_{14}$	$\text{C}_{26}\text{H}_{26}\text{CdN}_4\text{O}_7$
Formula weight	795.07	1237.82	618.91
Crystal system	Triclinic	Monoclinic	Orthorhombic
Space group	$P\bar{1}$	$P2_1/n$	$Pna2_1$
<i>a</i> (Å)	5.1741(8)	15.9628(9)	9.0634(5)
<i>b</i> (Å)	10.3722(16)	18.7238(10)	16.9571(10)
<i>c</i> (Å)	15.508(2)	16.6373(9)	16.8283(9)
$\alpha$ (°)	77.901(1)	90	90
$\beta$ (°)	81.973(2)	93.667(1)	90
$\gamma$ (°)	78.507(1)	90	90
<i>V</i> (Å <sup>3</sup> )	793.3(2)	4962.4(5)	2586.3(3)
<i>Z</i>	1	4	4
<i>D</i> <sub>calc</sub> (g cm <sup>-3</sup> )	1.664	1.657	1.589
$\mu$ (mm <sup>-1</sup> )	0.759	0.935	0.897
Min./max. trans.	0.8342/0.9071	0.8214/0.8865	0.8229/0.9284
<i>hkl</i> ranges	$-6 \leq h \leq 6$ , $-12 \leq k \leq 12$ , $-18 \leq l \leq 18$	$-19 \leq h \leq 16$ , $-22 \leq k \leq 22$ , $-20 \leq l \leq 20$	$-9 \leq h \leq 10$ , $-20 \leq k \leq 20$ , $-20 \leq l \leq 20$
Total reflections	11 324	30 514	15 187
Unique reflections	2 895	8 973	4 608
<i>R</i> (int)	0.0558	0.0450	0.0497
Parameters/restraints	251/0	697/6	349/4
<i>R</i> <sub>1</sub> (all data) <sup>a</sup>	0.0381	0.0478	0.0384
<i>R</i> <sub>1</sub> ( $I > 2\sigma(I)$ ) <sup>a</sup>	0.0379	0.0421	0.0346
<i>wR</i> <sub>2</sub> (all data) <sup>b</sup>	0.1015	0.1255	0.0850
<i>wR</i> <sub>2</sub> ( $I > 2\sigma(I)$ ) <sup>b</sup>	0.1012	0.1192	0.0822
Max./min. residual (e <sup>-</sup> /Å <sup>3</sup> )	0.798/−0.855	1.348/−1.457	0.794/−0.749
G.O.F.	1.119	1.056	1.088

<sup>a</sup>  $R_1 = \sum ||F_o| - |F_c|| / \sum |F_o|$ .

<sup>b</sup>  $wR_2 = \{ \sum [w(F_o^2 - F_c^2)]^2 / \sum [wF_o^2]^2 \}^{1/2}$ .

**Table 2**  
Bond length (Å) and angle (°) data for **1**.

Cd1–N1	2.307(3)	O3–Cd1–O3 <sup>#2</sup>	180
Cd1–O3	2.320(2)	N1–Cd1–O4 <sup>#1</sup>	85.14(8)
Cd1–O4 <sup>#1</sup>	2.371(2)	O3–Cd1–O4 <sup>#1</sup>	91.20(8)
N1–Cd1–N1 <sup>#2</sup>	180	N1–Cd1–O4 <sup>#3</sup>	94.86(8)
N1–Cd1–O3	93.87(8)	O3–Cd1–O4 <sup>#3</sup>	88.80(8)
N1–Cd1–O3 <sup>#2</sup>	86.13(8)	O4 <sup>#1</sup> –Cd1–O4 <sup>#3</sup>	180

Symmetry equivalent positions: #1,  $x - 1, y, z$ ; #2,  $-x + 2, -y, -z + 2$ ; #3,  $-x + 3, -y, -z + 2$ .

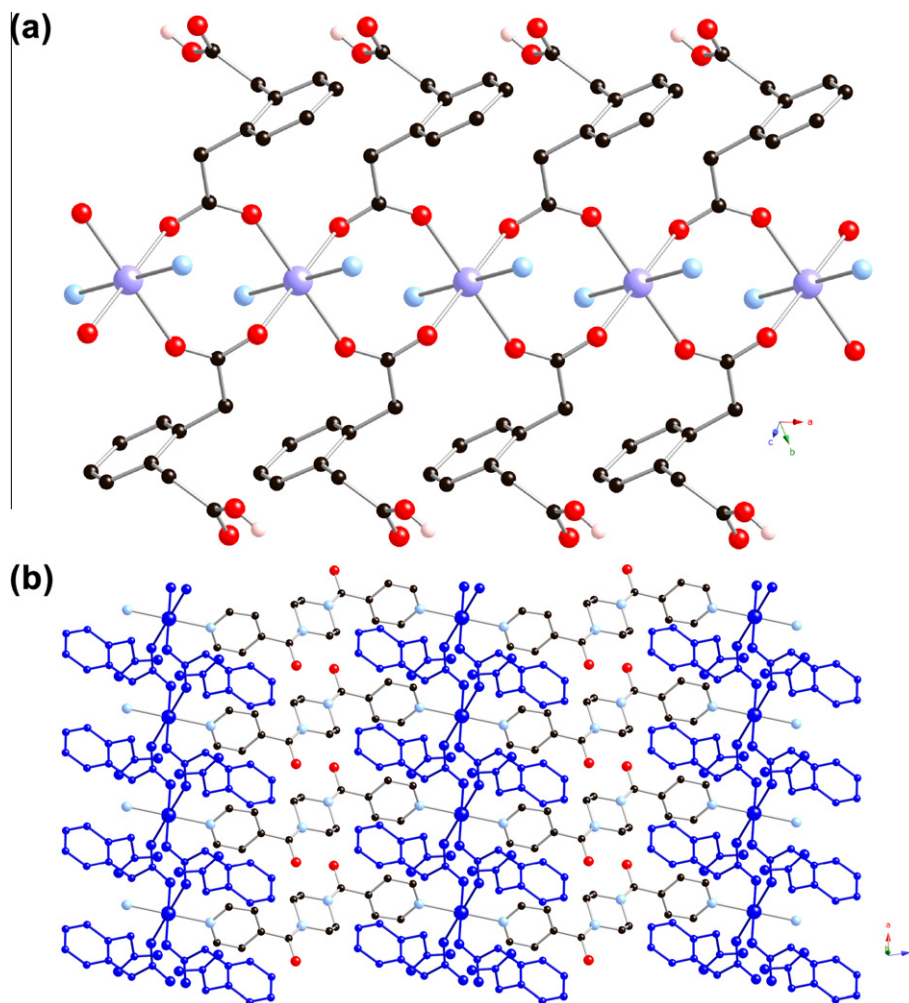


Fig. 1. (a)  $[\text{Cd}(1,2\text{-Hphda})_2]_n$  ribbon in **1**, with embedded  $[\text{Cd}(\text{OCO})_2]_n$  chain. (b)  $[\text{Cd}(1,2\text{-Hphda})_2(4\text{-bpfp})]_n$  layer in **1**.

Table 3

Hydrogen bonding distance (Å) and angle ( $^\circ$ ) data for **1–3**.

$D\text{-H}\cdots A$	$d(\text{H}\cdots A)$	$\angle\text{DHA}$	$d(D\cdots A)$	Symmetry transformation for A
<b>1</b>				
O1–H1A $\cdots$ O3	1.89	161.3	2.703(3)	$-x+3, -y-1, -z+2$
<b>2</b>				
O5–H5B $\cdots$ O10	1.99(2)	160(3)	2.783(3)	$-x+3/2, y-1/2, -z+5/2$
O5–H5A $\cdots$ O11	1.89(2)	165(3)	2.713(3)	$-x+1/2, y-1/2, -z+1/2$
O6–H6A $\cdots$ O14	1.82(2)	167(3)	2.656(3)	$-x+1, -y, -z+1$
O6–H6B $\cdots$ O13	1.89(2)	168(3)	2.712(3)	$-x, -y, -z$
<b>3</b>				
O7–H7A $\cdots$ O3	1.87(3)	158(5)	2.677(5)	$-x+1/2, y-1/2, z-1/2$
O7–H7B $\cdots$ O2	1.83(2)	179(5)	2.670(5)	$x-1/2, -y+3/2, z$

connected into  $[\text{Cd}(1,3\text{-phda})(4\text{-bpfp})(\text{H}_2\text{O})]_n$  coordination polymer (4,4) layers by tethering 4-bpfp ligands, which provide Cd $\cdots$ Cd distances of 16.637 Å (c lattice parameter). The full span of the 1,3-phda ligands, compared to the bridging carboxylate groups of the 1,2-Hphda ligands in **1**, provides substantially longer Cd $\cdots$ Cd distances in **2**. As a result, the larger grid windows permit parallel 2-fold interpenetration of crystallographically independent  $[\text{Cd}(1,3\text{-phda})(4\text{-bpfp})(\text{H}_2\text{O})]_n$  layers (Fig. 3). The grid apertures are significant more pinched than in **1**, with Cd $\cdots$ Cd $\cdots$ Cd angles of 129.8/50.4 $^\circ$ , and 129.4/50.6 $^\circ$ , within the two different layer motifs. Aggregation into the pseudo 3-D crystal structure of **2** (Fig. S4) occurs by hydrogen bonding donation from the aqua ligands in one interpenetrated layer

Table 4

Bond length (Å) and angle ( $^\circ$ ) data for **2**.

Cd1–O13	2.266(3)	Cd2–O14	2.233(2)
Cd1–O6	2.339(3)	Cd2–O5	2.355(2)
Cd1–O11 $^{\#1}$	2.371(3)	Cd2–O10 $^{\#3}$	2.361(3)
Cd1–N7 $^{\#2}$	2.380(3)	Cd2–N8 $^{\#2}$	2.368(3)
Cd1–N1	2.383(3)	Cd2–N4	2.384(3)
Cd1–O12 $^{\#1}$	2.399(2)	Cd2–O8 $^{\#3}$	2.384(2)
Cd1–O9	2.598(2)		
O13–Cd1–O6	84.34(8)	O14–Cd2–O5	91.82(9)
O13–Cd1–O11 $^{\#1}$	168.78(9)	O14–Cd2–O10 $^{\#3}$	171.81(8)
O6–Cd1–O11 $^{\#1}$	84.48(7)	O5–Cd2–O10 $^{\#3}$	83.89(8)
O13–Cd1–N7 $^{\#2}$	90.01(10)	O14–Cd2–N8 $^{\#2}$	83.29(9)
O6–Cd1–N7 $^{\#2}$	84.42(8)	O5–Cd2–N8 $^{\#2}$	89.05(9)
O11 $^{\#1}$ –Cd1–N7 $^{\#2}$	89.78(10)	O10 $^{\#3}$ –Cd2–N8 $^{\#2}$	89.64(9)
O13–Cd1–N1	89.60(10)	O14–Cd2–N4	87.58(9)
O6–Cd1–N1	88.13(8)	O5–Cd2–N4	83.32(8)
O11 $^{\#1}$ –Cd1–N1	89.16(10)	O10 $^{\#3}$ –Cd2–N4	98.82(9)
N7 $^{\#2}$ –Cd1–N1	172.55(10)	N8 $^{\#2}$ –Cd2–N4	167.91(10)
O13–Cd1–O12 $^{\#1}$	136.40(8)	O14–Cd2–O8 $^{\#3}$	130.76(8)
O6–Cd1–O12 $^{\#1}$	138.34(7)	O5–Cd2–O8 $^{\#3}$	136.16(8)
O11 $^{\#1}$ –Cd1–O12 $^{\#1}$	54.78(7)	O10 $^{\#3}$ –Cd2–O8 $^{\#3}$	55.08(7)
N7 $^{\#2}$ –Cd1–O12 $^{\#1}$	86.91(9)	N8 $^{\#2}$ –Cd2–O8 $^{\#3}$	103.90(9)
N1–Cd1–O12	98.49(8)	N4–Cd2–O8 $^{\#3}$	88.06(9)
O13–Cd1–O9	53.10(8)		
O6–Cd1–O9	135.15(7)		
O11 $^{\#1}$ –Cd1–O9	137.34(8)		
N7 $^{\#2}$ –Cd1–O9	106.46(9)		
N1–Cd1–O9	79.15(9)		
O12 $^{\#1}$ –Cd1–O9	86.32(8)		

Symmetry equivalent positions:  $\#1, x+1/2, -y+1/2, z+1/2$ ;  $\#2, x, y, z+1$ ;  $\#3, x-1/2, -y+1/2, z-1/2$ .

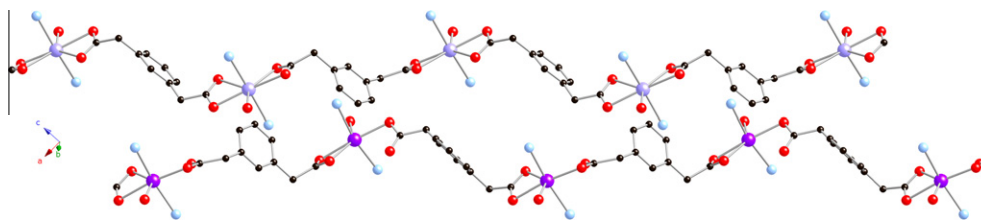


Fig. 2. Zig-zag  $[\text{Cd}(1,3\text{-phda})(\text{H}_2\text{O})]_n$  chains in **2**. 1,3-phda ligands in the top and bottom chains adopt bis(chelating) and monodentate/chelating binding modes, respectively.

to ligated carboxylate oxygen atoms belonging to the interpenetrated layers above and below.

Despite their common layered topology, compound **2** and its 4-bpmp analog  $[\text{Cd}(1,3\text{-phda})(4\text{-bpmp})]_n$  exhibit stark structural differences [23]. The latter material possesses (4,4) grids based on  $\{\text{Cd}_2\text{O}_2\}$  dimeric units and exotridentate 1,3-phda ligands, and lacks any interpenetration. It is plausible that the inclusion of aqua ligands in **2** alters the binding mode of the 1,3-phda carboxylate groups and therefore the overall coordination polymer topology.

#### 4.4. Structural description of $[\text{Cd}(1,4\text{-phda})(4\text{-bpfp})(\text{H}_2\text{O})]_n$ (**3**)

Compound **3** crystallizes in an acentric space group with an asymmetric unit containing a divalent cadmium atom, a fully deprotonated 1,4-phda ligand, a 4-bpfp ligand, and an aqua ligand (Fig. S5). The cadmium atom displays a distorted  $\{\text{CdN}_2\text{O}_5\}$  pentagonal bipyramidal geometry, with *trans* 4-bpfp pyridyl nitrogen donors in the axial positions. The equatorial plane is filled by an aqua ligand and chelating carboxylate groups from two 1,4-phda ligands. Bond parameters within the coordination environment in **3** are listed in Table 5.

Cadmium ions are connected by “staple” configuration 1,4-phda ligands ( $\text{C}-\text{C}\cdots\text{C}-\text{C}$  torsion angle =  $38.6^\circ$ ) in a bis(chelating) bind-

Table 5  
Bond length (Å) and angle ( $^\circ$ ) data for **3**.

Cd1–O7	2.253(3)	O7–Cd1–N3	84.27(14)
Cd1–O5	2.274(3)	O5–Cd1–N3	86.44(12)
Cd1–N4 <sup>#1</sup>	2.362(4)	N4 <sup>#1</sup> –Cd1–N3	175.45(13)
Cd1–O3 <sup>#2</sup>	2.364(4)	O3 <sup>#2</sup> –Cd1–N3	86.76(14)
Cd1–N3	2.412(4)	O7–Cd1–O4 <sup>#2</sup>	140.82(12)
Cd1–O4 <sup>#2</sup>	2.467(3)	O5–Cd1–O4 <sup>#2</sup>	86.87(11)
Cd1–O2	2.563(4)	N4 <sup>#1</sup> –Cd1–O4 <sup>#2</sup>	79.46(12)
O7–Cd1–O5	132.26(12)	O3 <sup>#2</sup> –Cd1–O4 <sup>#2</sup>	53.84(11)
O7–Cd1–N4 <sup>#1</sup>	91.40(13)	N3–Cd1–O4 <sup>#2</sup>	103.02(13)
O5–Cd1–N4 <sup>#1</sup>	97.55(12)	O7–Cd1–O2	80.66(11)
O7–Cd1–O3 <sup>#2</sup>	88.90(12)	O5–Cd1–O2	53.41(10)
O5–Cd1–O3 <sup>#2</sup>	137.15(11)	N4 <sup>#1</sup> –Cd1–O2	86.79(12)
N4 <sup>#1</sup> –Cd1–O3 <sup>#2</sup>	91.74(13)	O3 <sup>#2</sup> –Cd1–O2	169.41(11)
O4 <sup>#2</sup> –Cd1–O2	135.80(11)	N3–Cd1–O2	93.90(13)

Symmetry equivalent positions: #1,  $x, y, z - 1$ ; #2,  $-x, -y + 2, z - 1/2$ .

ing mode to produce  $[\text{Cd}(1,4\text{-phda})(\text{H}_2\text{O})]_n$  chains aligned along the  $[001]$  crystal direction (Fig. 4a) and coincident with the crystallographic  $2_1$  screw axes. The  $\text{Cd}\cdots\text{Cd}$  through-ligand distance is 9.623 Å. Despite the *para* disposition of the acetate pendant arms within the 1,4-phda ligands, the “staple” configuration enforces a shorter metal–metal contact distance than seen for the *meta* dicar-

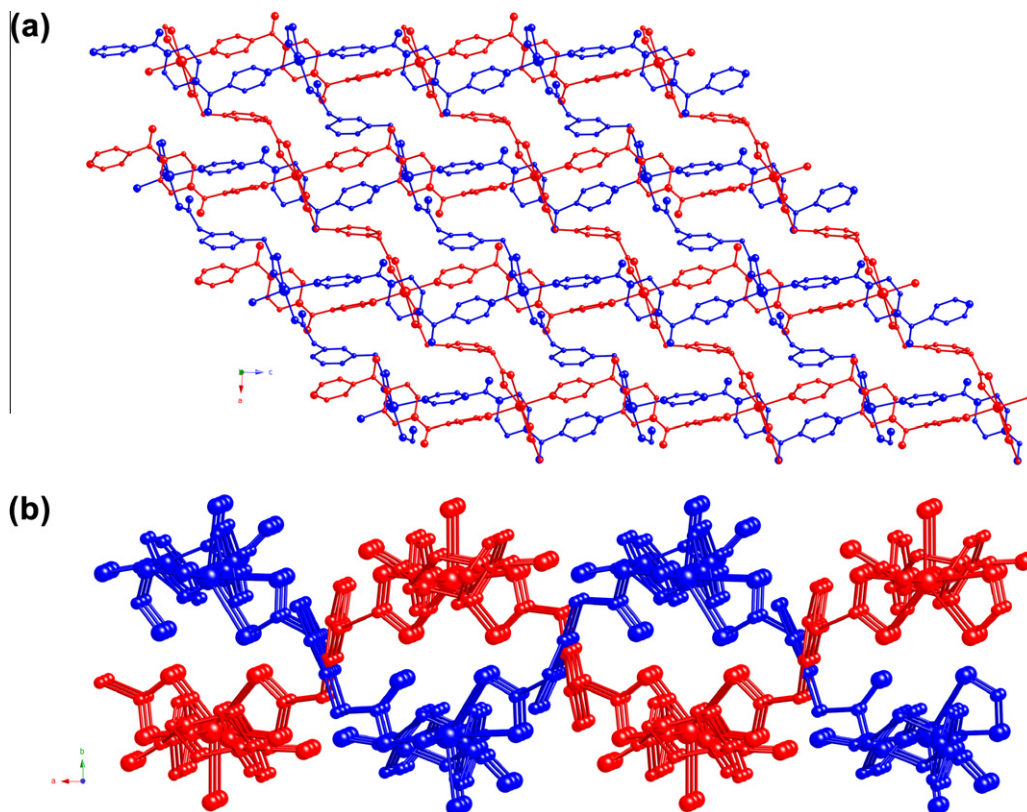


Fig. 3. Parallel 2-fold interpenetration of  $[\text{Cd}(1,3\text{-phda})(4\text{-bpfp})(\text{H}_2\text{O})]_n$  layers in **3**. (a) Face view. (b) Side view.

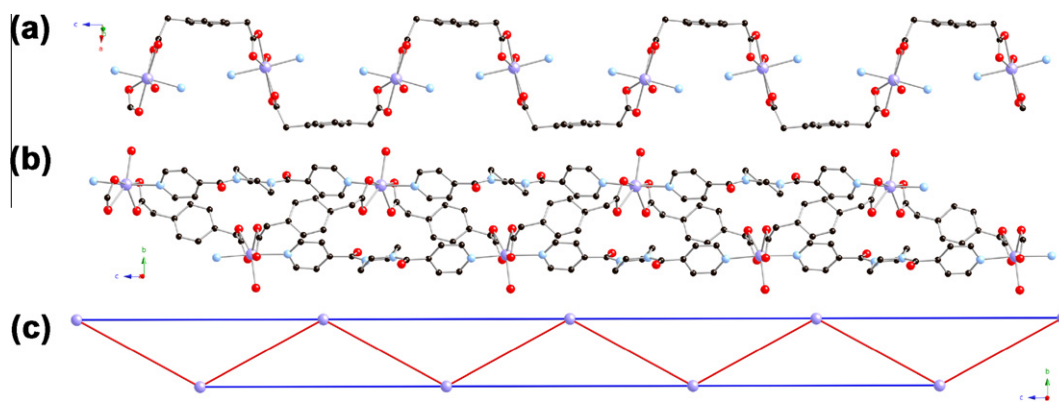


Fig. 4. (a)  $[\text{Cd}(1,4\text{-phda})(\text{H}_2\text{O})]_n$  chain in **3**. (b) 4-connected  $[\text{Cd}(1,4\text{-phda})(4\text{-bpfp})(\text{H}_2\text{O})]_n$  1-D chains in **3**. (c) Schematic representation of the  $3^3 4^2 5$  chain topology.

boxylate 1,3-phda ligands in **2**. Next nearest neighbor Cd atoms ( $\text{Cd}\cdots\text{Cd}$  distance = 16.835 Å) within these chains are bridged by 4-bpfp ligands (Fig. 4b). Thus the resulting  $[\text{Cd}(1,4\text{-phda})(4\text{-bpfp})(\text{H}_2\text{O})]_n$  1-D chains in **3** stand in direct contrast with the non-interpenetrated 2-D layers in **1** and 2-fold interpenetrated 2-D layers in **2**. The topology of the 1-D chain motifs in **3** can be determined by considering each cadmium ion as a 4-connected node with all ligands as simple linkers. According to TOPOS software [24], this treatment produces a 4-connected chain with  $3^3 4^2 5$  topology (Fig. 4c). Adjacent  $[\text{Cd}(1,4\text{-phda})(4\text{-bpfp})(\text{H}_2\text{O})]_n$  1-D chains aggregate by hydrogen bonding donation from aqua ligands to ligated 1,4-phda carboxylate oxygen atoms (Fig. S6).

The 1-D topology of compound **3** stands in marked contrast with the 2-D structure of its 4-bpmp analog  $\{[\text{Cd}(1,4\text{-phda})(4\text{-bpmp})] \cdot 1.5\text{H}_2\text{O}\}_n$  [23]. The latter material possesses  $[\text{Cd}(1,4\text{-phda})]$  double chains containing  $\{\text{Cd}_2\text{O}_2\}$  dimeric units and exotridentate 1,4-phda ligands, pillared into 2-D by 4-bpmp tethers. As in the aforementioned 1,3-phda derivative **2**, it is likely that the presence of bound water molecules in **3** affects the carboxylate binding mode and overall coordination polymer topology.

#### 4.5. Luminescent properties

Polycrystalline samples of **1–3** all underwent visible light fluorescence upon excitation with ultraviolet light ( $\lambda_{\text{ex}}$  values: **1**, 315 nm; **2**, 390 nm; **3**, 330 nm). Emission spectra are shown in Fig. 5. The emission spectrum of **1** shows two broad maxima, centered at 400 and 555 nm. According to a review of  $d^{10}$  metal coordination polymer luminescent behavior by Houk et al. [6a], the higher energy maximum is likely attributable to intraligand  $\pi\text{-}\pi^*$

or  $\pi\text{-}n$  transitions within the phda and 4-bpfp ligands, while the lower energy band is perhaps best ascribed to ligand-to-metal charge transfer (LMCT) transitions potentially involving the *anti-syn* bridged carboxylate groups. These latter modes are apparently absent for **2** and **3**, which show single intraligand-based emission maxima at 470 and 440 nm, respectively.

#### 5. Conclusions

The geometric disposition of the acetate arms of phda ligands appears to play a critical role in structure direction during self-assembly of cadmium coordination polymers containing long 4-bpfp tethering ligands. *Ortho* disposed acetate arms in 1,2-phda ligands promote 1-D *spiro*  $[\text{Cd}(\text{OCO})_2]$  ribbons, which are pillared into a standard (4,4) grid topology by the dipodal neutral tethers. A longer span between dicarboxylate termini in the 1,3-phda ligand resulted in larger grid apertures and a twofold parallel interpenetrated layered net. In the *para* substituted 1,4-phda derivative, the conformational flexibility of the acetate arms instills a helical twist and overall acentricity of the resulting 4-connected coordination polymer chains. The structural topologies of compound **2** and **3** differ greatly from those of their analogous bis(4-pyridylmethyl)piperazine derivatives, indicating a significant structure-directing effect via the 4-bpfp formyl groups and concomitant loss of lone pair electron density at the piperazinyll nitrogen atoms. Luminescent properties in this series appear to depend on the specific binding mode of the dicarboxylate ligands and coordination environment at cadmium. The results herein portend a potentially rich coordination polymer chemistry for the under-utilized 4-bpfp neutral tethering ligand.

#### Acknowledgements

The authors gratefully acknowledge the donors of the American Chemical Society Petroleum Research Fund for financial support of this work. C.Y.W. thanks Dr. Gail Richmond and the MSU High School Honors Science Program for his participation in the work, and thanks Dr. Ayasheed Mahpanzah for helpful discussions regarding the crystallography. We thank Ms. Amy Pochodylo for assistance with the fluorescence spectroscopy.

#### Appendix A. Supplementary material

Crystallographic data (excluding structure factors) for **1–3** have been deposited with the Cambridge Crystallographic Data Centre with Nos. 784854–784856, respectively. Copies of the data can be obtained free of charge via the Internet at <http://www.ccdc.cam.ac.uk/conts/retrieving.html>. Supplementary data associated

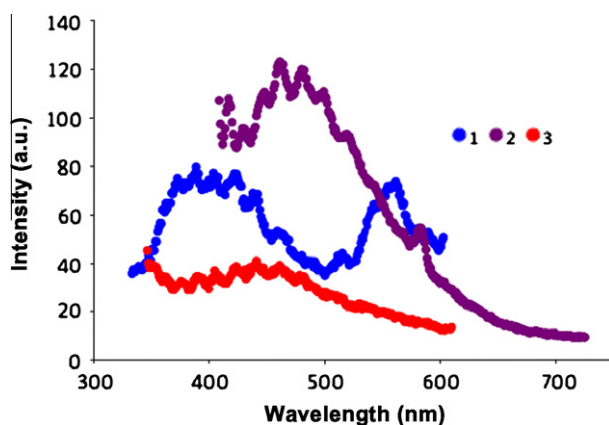


Fig. 5. Emission spectra of **1–3**.

with this article can be found, in the online version, at doi:10.1016/j.molstruc.2010.08.047.

## References

- [1] (a) A.U. Czaja, N. Trukhan, U. Mueller, *Chem. Soc. Rev.* 38 (2009) 1284, and references therein;  
 (b) C. Janiak, *Dalton Trans.* (2003) 2781, and references therein;  
 (c) U. Mueller, M. Schubert, F. Teich, H. Puetter, K. Schierle-Arndt, J. Pastré, *J. Mater. Chem.* 16 (2006) 626.
- [2] (a) S.S. Han, J.L. Mendoza-Cortes, W.A. Goddard III, *Chem. Soc. Rev.* 38 (2009) 1460, and references therein;  
 (b) L. Pan, D.H. Olson, L.R. Ciemmolowski, R. Heddy, J. Li, *Angew. Chem. Int. Ed.* 45 (2006) 616;  
 (c) M. Dinca, A.F. Yu, J.R. Long, *J. Am. Chem. Soc.* 128 (2006) 8904;  
 (d) J.L.C. Roswell, O.M. Yaghi, *Angew. Chem. Int. Ed.* 44 (2005) 4670;  
 (e) R. Matsuda, R. Kitaura, S. Kitagawa, Y. Kubota, R.V. Belosludov, T.C. Kobayashi, H. Sakamoto, T. Chiba, M. Takata, Y. Kawazoe, Y. Mita, *Nature* 436 (2005) 238;  
 (f) A.C. Sudik, A.R. Millward, N.W. Ockwig, A.P. Côté, J. Kim, O.M. Yaghi, *J. Am. Chem. Soc.* 127 (2005) 7110;  
 (g) X. Zhao, B. Xiao, A.J. Fletcher, K.M. Thomas, D. Bradshaw, M.J. Rosseinsky, *Science* 306 (2004) 1012;  
 (h) G. Férey, M. Latroche, C. Serre, F. Millange, T. Loiseau, A. Percheron-Guegan, *Chem. Commun.* (2003) 2976.
- [3] (a) J.-R. Li, R.J. Kuppler, H.-C. Zhou, *Chem. Soc. Rev.* 38 (2009) 1477, and references therein;  
 (b) S. Galli, N. Masciocchi, G. Tagliabue, A. Sironi, J.A.R. Navarro, J.M. Salas, L. Mendez-Liñan, M. Domingo, M. Perez-Mendoza, E. Barea, *Chem. Eur. J.* 14 (2008) 9890;  
 (c) J.S. Seo, D. Whang, H. Lee, S.I. Jun, J. Oh, Y.J. Jeon, K. Kim, *Nature* 404 (2000) 982.
- [4] (a) Q.-R. Fang, G.-S. Zhu, M. Xue, J.-Y. Sun, S.-L. Qiu, *Dalton Trans.* (2006) 2399;  
 (b) X.-M. Zhang, M.-L. Tong, H.K. Lee, X.-M. Chen, *J. Solid State Chem.* 160 (2001) 118;  
 (c) O.M. Yaghi, H. Li, T.L. Groy, *Inorg. Chem.* 36 (1997) 4292.
- [5] (a) J.Y. Lee, O.K. Farha, J. Roberts, K.A. Scheidt, S.T. Nguyen, J.T. Hupp, *Chem. Soc. Rev.* 38 (2009) 1450, and references therein;  
 (b) L. Ma, C. Abney, W. Lin, *Chem. Soc. Rev.* 38 (2009) 1248, and references therein;  
 (c) S.G. Baca, M.T. Reetz, R. Goddard, I.G. Philippova, Y.A. Simonov, M. Gdaniec, N. Gerbelevu, *Polyhedron* 25 (2006) 1215;  
 (d) H. Han, S. Zhang, H. Hou, Y. Fan, Y. Zhu, *Eur. J. Inorg. Chem.* 8 (2006) 1594;  
 (e) C.-D. Wu, A. Hu, L. Zhang, W. Lin, *J. Am. Chem. Soc.* 127 (2005) 8940;  
 (f) W. Mori, S. Takamizawa, C.N. Kato, T. Ohmura, T. Sato, *Micropor. Mesopor. Mater.* 73 (2004) 31;  
 (g) N. Guillou, Q. Gao, P.M. Forster, J.S. Chang, M. Noguès, S.-E. Park, G. Férey, A.K. Cheetham, *Angew. Chem. Int. Ed.* 40 (2001) 2831.
- [6] (a) M.D. Allendorf, C.A. Bauer, R.K. Bhakta, R.J.T. Houk, *Chem. Soc. Rev.* 38 (2009) 1330, and references therein;  
 (b) J. He, J. Yu, Y. Zhang, Q. Pan, R. Xu, *Inorg. Chem.* 44 (2005) 9279;  
 (c) S. Wang, Y. Hou, E. Wang, Y. Li, L. Xu, J. Peng, S. Liu, C. Hu, *New J. Chem.* 27 (2003) 1144;  
 (d) L.G. Beauvais, M.P. Shores, J.R. Long, *J. Am. Chem. Soc.* 122 (2000) 2763.
- [7] (a) S. Zang, Y. Su, Y. Li, Z. Ni, Q. Meng, *Inorg. Chem.* 45 (2006) 174;  
 (b) L. Wang, M. Yang, G. Li, Z. Shi, S. Feng, *Inorg. Chem.* 45 (2006) 2474.
- [8] (a) M. Eddaoudi, J. Kim, N. Rosi, D. Vodak, J. Wachter, M. O'Keefe, O.M. Yaghi, *Science* 295 (2002) 469;  
 (b) X.-N. Cheng, W.-X. Zhang, Y.-Y. Lin, Y.-Z. Zheng, X.-M. Chen, *Adv. Mater.* 19 (2007) 1494.
- [9] J. Tao, M.L. Tong, X.M. Chen, *J. Chem. Soc. Dalton Trans.* (2000) 3669.
- [10] D.J. Tranchemontagne, J.L. Mendoza-Cortés, M. O'Keefe, O.M. Yaghi, *Chem. Soc. Rev.* 38 (2009) 1257, and references therein.
- [11] (a) Y. Dai, E. Ma, E. Tang, J. Zhang, Z. Li, X. Huang, Y. Yao, *Cryst. Growth Des.* 5 (2005) 1313;  
 (b) N.L. Rosi, J. Eckert, M. Eddaoudi, D.T. Vodak, J. Kim, M. O'Keefe, O.M. Yaghi, *Science* 300 (2003) 1127;  
 (c) S. Zhu, H. Zhang, Y. Zhao, M. Shao, Z. Wang, M. Li, *J. Mol. Struct.* 892 (2008) 420.
- [12] X.-F. Xie, S.-P. Chen, Z.-Q. Xia, S.-L. Gao, *Polyhedron* 28 (2009) 679.
- [13] F. Yang, Y. Ren, D. Li, F. Fu, G. Qi, Y. Wang, *J. Mol. Struct.* 892 (2008) 283.
- [14] Z. Su, S.S. Chen, J. Fan, M.S. Chen, Y. Zhao, W.Y. Sun, *Cryst. Growth Des.* 10 (2010) 3675.
- [15] K.M. Blake, L.L. Johnston, J.H. Nettleman, R.M. Supkowski, R.L. LaDuca, *Cryst. Eng. Commun.* 12 (2010) 1927.
- [16] M.A. Braverman, R.L. LaDuca, *Cryst. Growth Des.* 7 (2007) 2343.
- [17] H. Hou, Y. Song, H. Xu, Y. Wei, Y. Fan, Y. Zhu, L. Li, C. Du, *Macromolecules* 36 (2003) 999.
- [18] Z.M. Wilseck, C.M. Gandolfo, R.L. LaDuca, *Inorg. Chim. Acta*, in press. doi: 10.1016/j.ica.2010.07.045.
- [19] SAINT, Software for Data Extraction and Reduction, Version 6.02 Bruker AXS, Inc.: Madison, WI, 2002.
- [20] SADABS, Software for Empirical Absorption Correction. Version 2.03 Bruker AXS, Inc.: Madison, WI, 2002.
- [21] G.M. Sheldrick, SHELXTL, Program for Crystal Structure Refinement, University of Göttingen: Göttingen, Germany, 1997.
- [22] H.D. Flack, *Acta Crystallogr. A* 29 (1983) 876.
- [23] K.M. Blake, G.A. Farnum, L.L. Johnston, R.L. LaDuca, *Inorg. Chim. Acta* 363 (2010) 88.
- [24] V.A. Blatov, A.P. Shevchenko, V.N. Serezhkin, *J. Appl. Crystallogr.* 33 (2000) 1193.